Coupled cavity terahertz quantum cascade lasers with integrated emission monitoring

Michael Krall,[1,3,4,*] Michael Martl,[1,3,4] Dominic Bachmann,[1,3] Christoph Deutsch,[1,3] Aaron M. Andrews,[2,3] Werner Schrenk,[3] Gottfried Strasser,[2,3] and Karl Unterrainer[1,3]

[1]*Photonics Institute, Vienna University of Technology, Gußhausstraße 27-29, 1040 Vienna, Austria*
[2]*Institute of Solid State Electronics, Vienna University of Technology, Floragasse 7, 1040 Vienna, Austria*
[3]*Center for Micro- and Nanostructures, Vienna University of Technology, Floragasse 7, 1040 Vienna, Austria*
[4]*These authors contributed equally to this work*
[*]*michael.krall@tuwien.ac.at*

Abstract: We demonstrate the on-chip generation and detection of terahertz radiation in coupled cavity systems using a single semiconductor heterostructure. Multiple sections of a terahertz quantum cascade laser structure in a double-metal waveguide are optically coupled and operate either as a laser or an integrated emission monitor. A detailed analysis of the photon-assisted carrier transport in the active region below threshold reveals the detection mechanism for photons emitted by the very same structure above threshold. Configurations with a single laser cavity and two coupled laser cavities are studied. It is shown that the integrated detector can be used for spatial sensing of the light intensity within a coupled cavity.

©2015 Optical Society of America

OCIS codes: (140.3945) Microcavities; (140.5965) Semiconductor lasers, quantum cascade; (250.0040) Detectors; (250.3140) Integrated optoelectronic circuits; (260.3090) Infrared, far.

References and links

1. J. Faist, F. Capasso, D. L. Sivco, C. Sirtori, A. L. Hutchinson, and A. Y. Cho, "Quantum cascade laser," Science **264**(5158), 553–556 (1994).
2. A. Lyakh, R. Maulini, A. Tsekoun, R. Go, and C. K. N. Patel, "Intersubband absorption of quantum cascade laser structures and its application to laser modulation," Appl. Phys. Lett. **92**(21), 211108 (2008).
3. M. Liertzer, L. Ge, A. Cerjan, A. D. Stone, H. E. Türeci, and S. Rotter, "Pump-induced exceptional points in lasers," Phys. Rev. Lett. **108**(17), 173901 (2012).
4. M. Brandstetter, M. Liertzer, C. Deutsch, P. Klang, J. Schöberl, H. E. Türeci, G. Strasser, K. Unterrainer, and S. Rotter, "Reversing the pump dependence of a laser at an exceptional point," Nat Commun **5**, 4034 (2014).
5. G. Fasching, Ch. Deutsch, A. Benz, A. M. Andrews, P. Klang, R. Zobl, W. Schrenk, G. Strasser, P. Ragulis, V. Tamosiūnas, and K. Unterrainer, "Electrically controllable photonic molecule laser," Opt. Express **17**(22), 20321–20326 (2009).
6. C. Mauro, R. P. Green, A. Tredicucci, F. Beltram, H. E. Beere, and D. A. Ritchie, "Amplification of terahertz radiation in quantum cascade structures," J. Appl. Phys. **102**(6), 063101 (2007).
7. H. Li, J. M. Manceau, A. Andronico, V. Jagtap, C. Sirtori, L. H. Li, E. H. Linfield, A. G. Davies, and S. Barbieri, "Coupled-cavity terahertz quantum cascade lasers for single mode operation," Appl. Phys. Lett. **104**(24), 241102 (2014).
8. M. Martl, J. Darmo, C. Deutsch, M. Brandstetter, A. M. Andrews, P. Klang, G. Strasser, and K. Unterrainer, "Gain and losses in THz quantum cascade laser with metal-metal waveguide," Opt. Express **19**(2), 733–738 (2011).
9. D. Burghoff, T.-Y. Kao, D. Ban, A. W. M. Lee, Q. Hu, and J. Reno, "A terahertz pulse emitter monolithically integrated with a quantum cascade laser," Appl. Phys. Lett. **98**(6), 061112 (2011).
10. D. Hofstetter, M. Beck, and J. Faist, "Quantum-cascade-laser structures as photodetectors," Appl. Phys. Lett. **81**(15), 2683–2685 (2002).
11. L. Gendron, M. Carras, A. Huynh, V. Ortiz, C. Koeniguer, and V. Berger, "Quantum cascade photodetector," Appl. Phys. Lett. **85**(14), 2824–2826 (2004).
12. M. Graf, G. Scalari, D. Hofstetter, J. Faist, H. Beere, E. Linfield, D. Ritchie, and G. Davies, "Terahertz range quantum well infrared photodetector," Appl. Phys. Lett. **84**(4), 475–477 (2004).
13. B. Schwarz, P. Reininger, H. Detz, T. Zederbauer, A. M. Andrews, S. Kalchmair, W. Schrenk, O. Baumgartner, H. Kosina, and G. Strasser, "A bi-functional quantum cascade device for same-frequency lasing and detection," Appl. Phys. Lett. **101**(19), 191109 (2012).
14. B. Schwarz, P. Reininger, D. Ristanić, H. Detz, A. M. Andrews, W. Schrenk, and G. Strasser, "Monolithically integrated mid-infrared lab-on-a-chip using plasmonics and quantum cascade structures," Nat Commun **5**, 4085 (2014).

#229056 - $15.00 USD Received 4 Dec 2014; revised 9 Jan 2015; accepted 14 Jan 2015; published 5 Feb 2015
(C) 2015 OSA

15. A. Benz, M. Krall, S. Schwarz, D. Dietze, H. Detz, A. M. Andrews, W. Schrenk, G. Strasser, and K. Unterrainer, "Resonant metamaterial detectors based on THz quantum-cascade structures," Sci Rep **4**, 4269 (2014).
16. Y. L. Lim, P. Dean, M. Nikolić, R. Kliese, S. P. Khanna, M. Lachab, A. Valavanis, D. Indjin, Z. Ikonić, P. Harrison, E. H. Linfield, A. G. Davies, S. J. Wilson, and A. D. Rakić, "Demonstration of a self-mixing displacement sensor based on terahertz quantum cascade lasers," Appl. Phys. Lett. **99**(8), 081108 (2011).
17. F. R. Giorgetta, E. Baumann, M. Graf, Q. Yang, C. Manz, K. Kohler, H. E. Beere, D. A. Ritchie, E. Linfield, A. G. Davies, Y. Fedoryshyn, H. Jackel, M. Fischer, J. Faist, and D. Hofstetter, "Quantum cascade detectors," IEEE J. Quantum Electron. **45**(8), 1039–1052 (2009).
18. H. C. Liu, C. Y. Song, A. J. SpringThorpe, and J. C. Cao, "Terahertz quantum-well photodetector," Appl. Phys. Lett. **84**(20), 4068–4070 (2004).
19. Y. Chassagneux, Q. J. Wang, S. P. Khanna, E. Strupiechonski, J. Coudevylle, E. H. Linfield, A. G. Davies, F. Capasso, M. A. Belkin, and R. Colombelli, "Limiting factors to the temperature performance of THz quantum cascade lasers based on the resonant-phonon depopulation scheme," IEEE Trans. Terahertz Sci. Technol. **2**(1), 83–92 (2012).
20. R. Lake, G. Klimeck, R. C. Bowen, and D. Jovanovic, "Single and multiband modeling of quantum electron transport through layered semiconductor devices," J. Appl. Phys. **81**(12), 7845–7869 (1997).
21. L. E. Henrickson, "Nonequilibrium photocurrent modeling in resonant tunneling photodetectors," J. Appl. Phys. **91**(10), 6273–6281 (2002).
22. M. Krall, D. Bachmann, C. Deutsch, M. Brandstetter, H. Detz, A. M. Andrews, W. Schrenk, G. Strasser, and K. Unterrainer, "All-electrical thermal monitoring of terahertz quantum cascade lasers," IEEE Photon. Technol. Lett. **26**(14), 1470–1473 (2014).
23. H. Luo, H. C. Liu, C. Y. Song, and Z. R. Wasilewski, "Background-limited terahertz quantum-well photodetector," Appl. Phys. Lett. **86**(23), 231103 (2005).

1. Introduction

Coupled cavity systems based on quantum cascade laser (QCL) structures [1] have been studied for realizing integrated optical circuits in the mid-infrared and THz spectral range. Their applications range from on-chip optical modulation [2] to studying exceptional points in coupled lasers systems [3,4]. In the THz frequency region, pairs of microdisks with electrically controlled optical coupling have been investigated [4,5]. In the case of strong optical coupling, the emission from one cavity can be modulated by changing the gain or loss in the coupled cavity [5]. If the loss in one cavity is sufficiently large, even exceptional points can be observed, i.e. the system turns off although the pump power is increased [4]. In addition, coupled cavity systems have also been used for realizing integrated amplifier sections [6] and frequency selective elements [7].

In order to study the optical gain or loss in a THz QCL active region, coupled cavity configurations have been used to electrically separate an integrated THz emitter section from the device under test [8,9]. THz time-domain spectroscopy (TDS) experiments reveal the bias-dependent gain or loss spectra of the investigated gain medium. In particular, the structure can show strong absorption at the lasing frequency for a certain range of applied electric fields. This effect has been used to realize an integrated modulation scheme for a mid-infrared QCL [2]. The intersubband absorption that has been observed in THz TDS experiments [8] suggests to further investigate these effects in THz QCL structures for its potential use in realizing an integrated photodetector.

Photodetectors based on quantum cascade structures have been realized in the mid-infrared [10,11] and THz range [12]. For operating wavelengths above the Reststrahlen band, in the mid-infrared, the concept of a bi-functional quantum cascade device has been demonstrated [13]. It employs a quantum cascade structure that has been adapted to operate as a laser for a certain applied electric field, and as a photovoltaic detector at zero bias, sensing the emission frequency of the lasing structure. A decoupled detection of the emitted light over a distance of 50 μm has been achieved by implementing a plasmonic waveguide between laser and detector [14]. In the THz spectral range, it has been further demonstrated that a QCL active region can be utilized as a photodetector by coupling normal incident light with a resonant metamaterial to different intersubband transitions [15]. However, the detected frequency range differed from the emission frequency of the active region. In fact, photovoltaic detection was demonstrated for transitions above the Reststrahlen band.

In this work, we present a THz QCL structure that can be operated in a detector mode, measuring the optical emission of a laser cavity by an optically coupled photodetector section.

#229056 - $15.00 USD Received 4 Dec 2014; revised 9 Jan 2015; accepted 14 Jan 2015; published 5 Feb 2015
(C) 2015 OSA

It has to be noted that we use a standard quantum cascade laser design without any modifications [8]. In contrast to previous studies, where the THz detection process was based on a self-mixing effect [16], an electrically decoupled laser-detector system is employed. It is demonstrated that the detector can be used to monitor the optical emission of an optically coupled laser cavity during operation. We further show that for coupled laser systems such integrated detector sections can be used as local emission sensors.

2. THz quantum cascade laser structure as photodetecting medium

We study the photodetection capabilities of a four-well resonant phonon THz QCL design emitting at about 2 THz [8]. The quantum cascade structure has a layer sequence of **32**/97/**57**/84/**31**/70/**43**/163 Å with $Al_{0.15}Ga_{0.85}As$ barriers indicated by bold letters and GaAs wells. The doping is homogeneously applied to the widest well with a density of 3.5×10^{15} cm^{-3}. The optical gain and loss as a function of the applied electric field has been characterized using THz TDS [8]. The measured absorption at the lasing frequency below threshold is explained by the parasitic carrier injection into the lower laser level and the subsequent photon-assisted transition to the extractor state. This finding suggests the use of this absorption process for realizing an integrated photodetector. Unlike regular quantum cascade detector (QCD) and quantum well infrared photodetector (QWIP) schemes, where carriers in the lower state are inherently provided by the doping in the active well [10–12,17,18], the lower level population density of the utilized intersubband transition is adjusted by resonant carrier injection. However, similar to common QCD designs, the excited state is quickly depopulated as a result of the resonant phonon depopulation scheme.

Investigating the laser and detector operation of the quantum cascade structure requires a detailed analysis of the interaction between photons and electrons in the active region. In Fig. 1 the band structure is illustrated for two different applied electric fields. At a field of 4.8 kV/cm, as shown in Fig. 1(a), the injector state is in resonance with the lower lasing level. This is considered a parasitic current channel in THz QCL active region designs [19]. However, it is also a source of optical absorption and can be used to generate a photocurrent, i.e. carrier transport through the structure assisted by photon absorption. This is in contrast to the photon-assisted transport at the lasing design field of the structure, where the carrier transport is strongly enhanced by the stimulated emission of photons. Increasing the applied electric field to 8.7 kV/cm, as shown in Fig. 1(b), tunes the injector into resonance with the upper lasing level. The energy difference between upper and lower laser level at this point, corresponds to the laser emission frequency of about 2.1 THz.

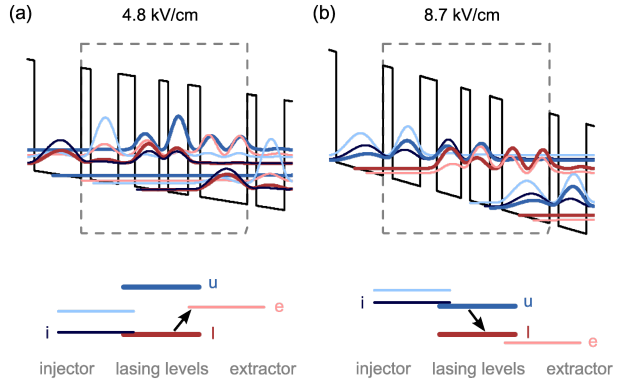

Fig. 1. Band structure and simplified sketch of the level alignment showing the relevant optical transitions at 2.1 THz. The quantum cascade heterostructure is operated (a) at a low bias field in the detector mode, or (b) above threshold in the laser mode.

#229056 - $15.00 USD Received 4 Dec 2014; revised 9 Jan 2015; accepted 14 Jan 2015; published 5 Feb 2015
(C) 2015 OSA

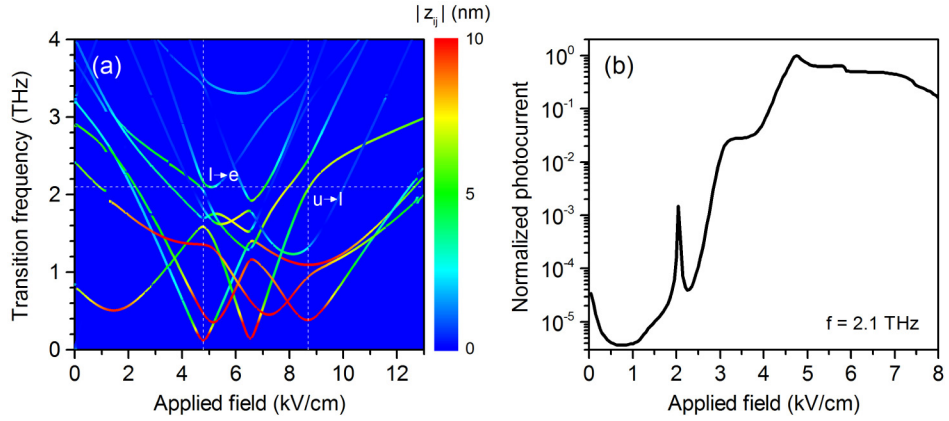

Fig. 2. (a) Calculated dipole moments for all relevant intersubband transitions as a function of the applied electric field. The horizontal dashed line indicates the design emission frequency (2.1 THz), and the two vertical lines indicate the detector (4.8 kV/cm) and laser (8.7 kV/cm) alignment fields. The respective dipole moments of the 2.1 THz transitions are 4.5 nm for the detector mode (l-e) and 6.3 nm for the laser mode (u-l). (b) Normalized photoresponse of the quantum cascade structure at 2.1 THz calculated using an NEGF-based quantum transport model.

In order to measure the emitted light of the lasing structure, the absorbing structure needs to be tuned in resonance with the energy of the emitted light. Figure 2(a) depicts the calculated dipole moments for all relevant intersubband transitions in the structure as a function of the applied electric field. At 4.8 kV/cm the transition from the lower lasing level to the extractor state is tuned in resonance with the transition frequency between the upper and lower laser levels at 8.7 kV/cm. A rigorous calculation of the photon-assisted current transport, however, also needs to include the population of the contributing energy levels and quantum transport mechanisms. In order to consider the carrier distribution in the structure, we use a non-equilibrium Green's function (NEGF) approach [20] to study the photoresponse at electric fields below the lasing threshold [21]. For the computation of the photoresponse we include the effect of photon-electron interaction on the electron transport in the device. The photocurrent below threshold is calculated in the linear regime, accounting for the full non-local electron-photon interaction in the self-consistent Born approximation. Figure 2(b) shows the calculated photoresponse of the quantum cascade structure depending on the applied electric field. Supporting the dipole moment estimation, the NEGF based transport model yields a maximum photocurrent for an electric field of approximately 4.8 kV/cm.

This concept of generating and detecting THz radiation at the same frequency is based on the QCL design scheme of resonant injection (extraction) of electrons into (from) the upper (lower) laser level and an efficient depopulation of the extractor state by longitudinal-optical phonon scattering. Therefore, this approach can also be similarly applied for other THz frequencies, where this design scheme can be used. However, it should be noted that the more injector or extractor states there are available, the easier it will be to match emission and detection frequencies.

3. Coupled cavities for integrated emission monitoring

The 16 µm thick quantum cascade structure was covered by Ti/Au metal layers on top and bottom, forming a double-metal waveguide. Due to its subwavelength dimension, coupling of externally generated THz radiation into the waveguide is very inefficient. One possibility to overcome this obstacle is to use a metamaterial on top of the active region [15]. This approach is especially useful for detecting normal incident light. However, in the case of on-chip light generation and detection, the detector element can be directly coupled to the laser section. We fabricated a coupled cavity system that consist of a short detector (QCD) section and a long laser (QCL) section as depicted in Fig. 3.

#229056 - $15.00 USD Received 4 Dec 2014; revised 9 Jan 2015; accepted 14 Jan 2015; published 5 Feb 2015
(C) 2015 OSA

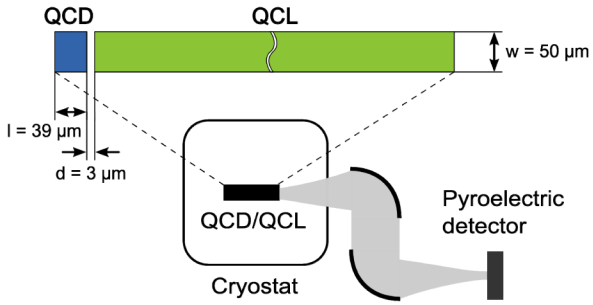

Fig. 3. Experimental configuration with a short detector (QCD) section optically coupled to a long laser (QCL) section. The emitted light is collected and measured for comparison also with an external pyroelectric detector.

The two optical cavities were defined using standard photolithography and reactive ion etching. In order to ensure optical coupling, but prevent electrical crosstalk between the sections, a gap of 3 µm was introduced between the two cavities [8]. On the one hand, the separation has to be large enough that the active region in the gap is completely removed during reactive ion etching ensuring that the two sections are fully electrically separated. On the other hand, a deep subwavelength spacing as small as possible ensures a strong optical coupling between the cavities, and therefore a high optical intensity in the detector and low outcoupling losses in the gap with respect to the laser operation. The devices were mounted in a continuous flow helium cryostat, and all measurements were performed at a constant heat sink temperature of 6 K. It has to be noted that for continuous-wave operation and large duty cycles the active region can heat up significantly [22], which may result in a thermal coupling between the two sections.

The two cavities were characterized independently by light-current-voltage (LIV) measurements using an external pyroelectric detector. As shown in Fig. 4(a), the laser section emits THz radiation for applied biases close to the design field of the structure, while the short detector section does not show any lasing. The difference in photon-assisted current transport above threshold is also clearly observed. While in the laser section the current density strongly increases due to stimulated emission, no such effect is observed in the short detector section, in which optical losses dominate over gain. In addition, the photon-assisted current transport in the lasing device is electrically stabilizing the active region, shifting the onset of the negative differential resistance region to a higher bias voltage. The emission spectrum of the laser section verifying the emission frequency of about 2.1 THz is shown in Fig. 4(b).

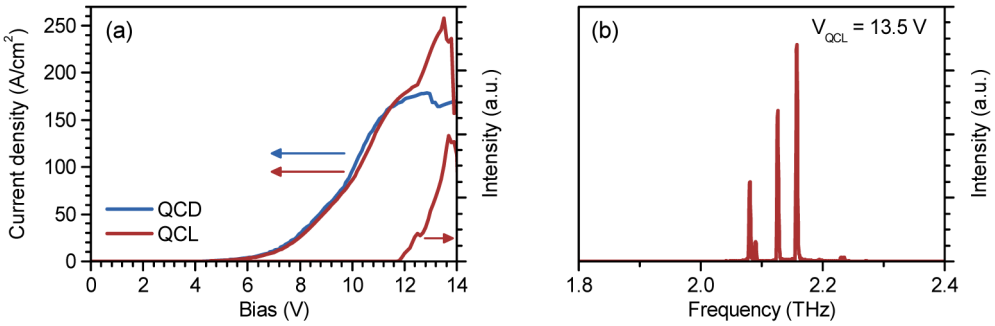

Fig. 4. (a) Light-current-voltage characterization of a non-lasing QCD section and a lasing QCL device at a heat sink temperature of 6 K. (b) Emission spectrum of the QCL section for an applied bias of 13.5 V.

#229056 - $15.00 USD Received 4 Dec 2014; revised 9 Jan 2015; accepted 14 Jan 2015; published 5 Feb 2015
(C) 2015 OSA

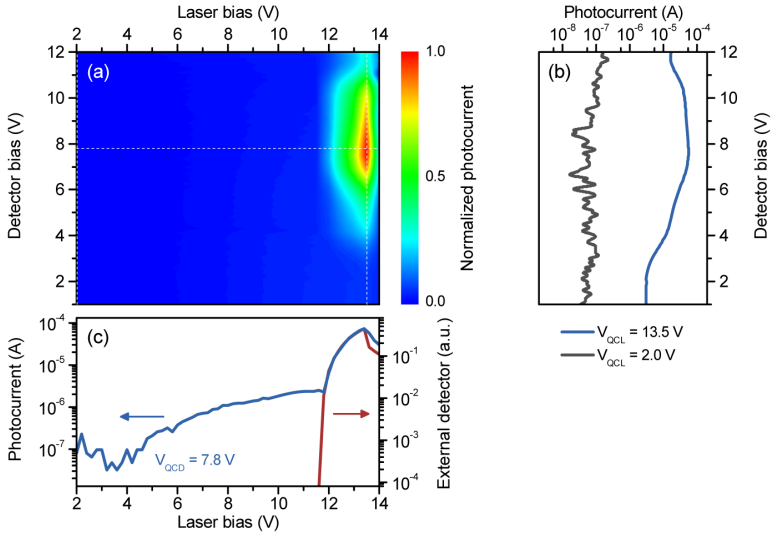

Fig. 5. (a) Two-dimensional bias dependence of the photo-induced current measured in the detector section. The laser cavity is operated in pulsed mode with a duty cycle of 10% (V_{QCL}) and a DC bias is applied to the detector section (V_{QCD}). The onset of lasing is clearly observed if the detector is tuned in resonance with the emission frequency. The maximum photoresponse is obtained with a detector bias of 7.8 V. (b) Cross sections for the QCL operating far below (V_{QCL} = 2 V) and above threshold (V_{QCL} = 13.5 V) are shown. (c) Comparison of the output intensity indicated by the measured photocurrent in the QCD and the signal from the external pyroelectric detector. The internal detector bias is kept constant (V_{QCD} = 7.8 V) and the output power is measured as a function of the laser bias.

The photo-induced current in the QCD as a function of the applied bias to the detector and the laser section is shown in Fig. 5(a). The QCL section was operated in pulsed mode with a duty cycle of 10% and the photocurrent in the detector section was measured using a lock-in amplifier. A strong increase of photocurrent is observed at the onset of stimulated emission in the laser cavity. The maximum photoresponse is achieved for a detector bias of V_{QCD} = 7.8 V, as shown in Fig. 5(b). This corresponds to an applied field of 4.9 kV/cm, which is in very good agreement with our simulation results. From the ratio of the measured photocurrent to the externally measured optical output power, we estimate a responsivity of ~6×10^{-2} A/W. This is about one order of magnitude above previous THz QCD results [12] and about one order of magnitude below values reported for THz QWIPs [23]. A direct comparison of the measured photocurrent with the signal generated by the external pyroelectric detector is shown in Fig. 5(c). The detector section was operated at its point of maximum responsivity. Above lasing threshold, the photoresponse of the detector section agrees very well with the output power measured by the pyroelectric detector. This clearly demonstrates the capability of the internal detector to monitor the emitted power of the laser cavity. Below threshold the induced current in the detector section is found to be proportional to the thermally dissipated power in the QCL section. Although the dark current is cancelled by the lock-in detection scheme, changes induced by the modulation (e.g. heating effects caused by the thermal coupling due to the common substrate) are still included.

4. Coupled laser systems with integrated detection

In addition, we studied a more complex configuration with two coupled laser cavities and an integrated detector element. The three-cavity configuration used for this experiment is shown in Fig. 6. It consists of two 1 mm long laser cavities and a 39 µm long detector section, each section separated by a gap of 3 µm.

#229056 - $15.00 USD Received 4 Dec 2014; revised 9 Jan 2015; accepted 14 Jan 2015; published 5 Feb 2015
(C) 2015 OSA

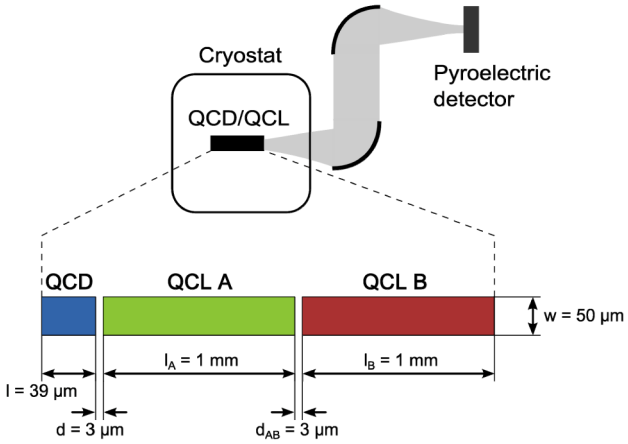

Fig. 6. Experimental configuration of a coupled laser system (QCL A, QCL B) with an integrated emission monitor (QCD). An external pyroelectric detector is used for reference purposes.

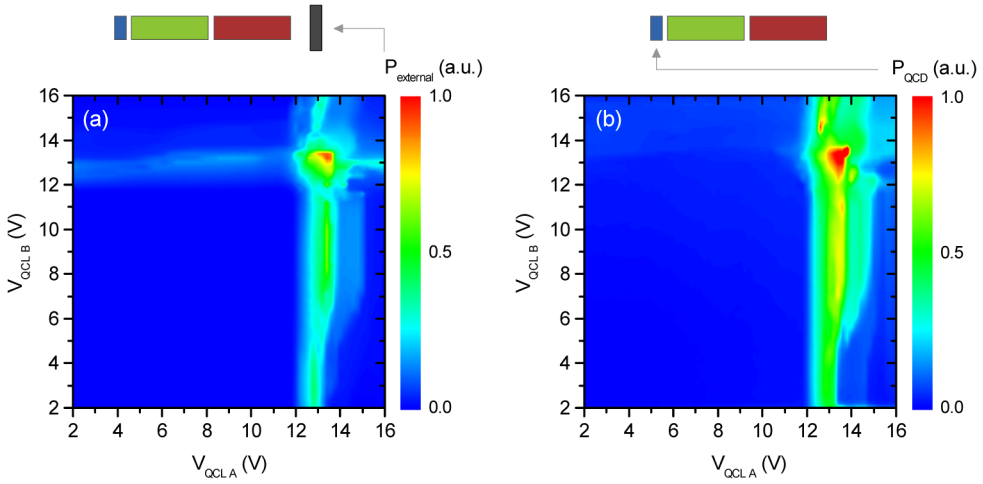

Fig. 7. Optical coupling between the two laser sections. The laser cavities are operated in pulsed mode with a duty cycle of 10%, and a constant bias of 7.8 V is applied to the detector section. (a) Output power measured with the external detector ($P_{external}$). (b) Photo-induced current within the detector section (P_{QCD}).

The bias dependent total output power of the two coupled laser cavities, which is shown in Fig. 7(a), was first measured with an external pyroelectric detector. The clearly visible mutual modulation of the total output power indicates the coupling of the two laser cavities. If the QCL sections A and B are equally biased above threshold, the total emitted power exceeds the sum of output powers of the two sections biased individually. This positive coupling effect can also be noticed in the increased bias range for lasing. In case one laser section is pumped above threshold and a low bias is applied to the other laser section, the emitted power decreases and exhibits a minimum around 5 V. This minimum agrees with the measured peak in losses due to intersubband absorption in the active region [8]. However, it also shows that the point of maximum absorption does not necessarily coincide with the point of maximum photoresponse. The fact that the amount of light collected from section A above threshold is greater than that of section B, results from unequal device performance of the two distinct laser sections and a higher collection efficiency of the output power emitted by section A.

#229056 - $15.00 USD Received 4 Dec 2014; revised 9 Jan 2015; accepted 14 Jan 2015; published 5 Feb 2015
(C) 2015 OSA

In order to investigate the short QCD section as an integrated photodetector for configurations with various coupled laser cavities, we compare the photocurrent in this section with the optical power measured by the external detector. The photocurrent was measured with a bias of 7.8 V applied to the detector section and is shown in Fig. 7(b). For section A biased above threshold the photocurrent measurement agrees very well with the externally detected output power of the coupled laser cavities in Fig. 7(a). If section A is biased below threshold, only a weak signal is registered by the internal detector. This can be explained by the weak coupling between QCL B and the detector section. The dependence of the signal from the internal monitor on the optical coupling strength with the respective laser cavity can therefore be used for the local sensing of the emission intensity, which is not possible using an external detection scheme.

5. Conclusion

In conclusion, we have demonstrated a THz quantum cascade laser structure that can be used as a monolithic integrated photodetector. The selection between detection and stimulated emission of THz radiation is achieved by changing the applied bias. In contrast to common design schemes for quantum cascade detectors, the presented detection element is not operated in a photovoltaic mode, but a certain electric field is applied to the quantum cascade structure in order to tune it into resonance with the emission frequency of the lasing element. The detection capabilities are demonstrated using a coupled cavity system with a regular laser section and a short optically coupled emission monitoring section. A very good agreement of the photo-induced current with the externally detected laser output power is observed. In addition, a direct use of such integrated emission monitoring is demonstrated with two coupled laser cavities. The integrated photodetector is not only able to measure the emitted power from the coupled laser cavity system, but it also allows the spatial sensing of the light intensity within the coupled cavity. The potential use of this intrinsically fast photon absorbing element ranges from emission monitoring to on-chip modulation. Therefore, the demonstrated approach can be applied for realizing complex photonic integrated circuits with on-chip generation, manipulation, and detection of light.

Acknowledgments

The authors acknowledge financial support by the Austrian Science Fund FWF (SFB IR-ON F25, SFB NextLite F49, DK CoQuS W1210, DK Solids4Fun W1243), the Austrian Nano Initiative project (PLATON), and the Austrian Society for Microelectronics (GMe). The authors would also like to thank Juraj Darmo for his encouragement and helpful discussions.

#229056 - $15.00 USD Received 4 Dec 2014; revised 9 Jan 2015; accepted 14 Jan 2015; published 5 Feb 2015
(C) 2015 OSA